

Low pressure line shape study of nitrogen-perturbed acetylene transitions in the $\nu 1 + \nu 3$ band over a range of temperatures

Chad Povey, Mileno Guillorel-Obregon, Adriana Predoi-Cross, Sergey V. Ivanov, Oleg G. Buzykin, Franck Thibault

▶ **To cite this version:**

Chad Povey, Mileno Guillorel-Obregon, Adriana Predoi-Cross, Sergey V. Ivanov, Oleg G. Buzykin, et al.. Low pressure line shape study of nitrogen-perturbed acetylene transitions in the $\nu 1 + \nu 3$ band over a range of temperatures. Revue canadienne de physique, 2013, 91 (11), pp.896-905. 10.1139/cjp-2013-0031 . hal-00971685

HAL Id: hal-00971685
https://hal.science/hal-00971685

Submitted on 11 Apr 2014

HAL is a multi-disciplinary open access archive for the deposit and dissemination of scientific research documents, whether they are published or not. The documents may come from teaching and research institutions in France or abroad, or from public or private research centers.

L'archive ouverte pluridisciplinaire **HAL**, est destinée au dépôt et à la diffusion de documents scientifiques de niveau recherche, publiés ou non, émanant des établissements d'enseignement et de recherche français ou étrangers, des laboratoires publics ou privés.

Low pressure line shape study of nitrogen perturbed acetylene transitions in the $\nu_1+\nu_3$ band over a range of temperatures

Chad Povey[1], Mileno Guillorel-Obregon[2], Adriana Predoi-Cross[1], Sergey V. Ivanov[3], Oleg G. Buzykin[4], Franck Thibault[2]

[1]Alberta Terrestrial Imaging Centre, Department of Physics and Astronomy, University of Lethbridge, 4401 University Drive, Lethbridge, AB, T1K 3M4 Canada, [2]Institut de Physique de Rennes, UMR CNRS 6251, Université de Rennes I, F-35042 Rennes, France, [3]Institute on Laser and Information Technologies, Russian Academy of Sciences, 2 Pionerskaya Str., 142190 Troitsk, Moscow Region, Russia, [4]Central Aerohydrodynamic Institute (TsAGI), 140160 Zhukovski, Moscow Region, Russia,

For Review Only

Number of manuscript pages: 14
Number of Figures: 9
Number of Tables: 5
Running Title:

Send correspondence to:
Dr. A. Predoi-Cross
Department of Physics and Astronomy, University of Lethbridge, 4401 University Drive, Lethbridge, AB, T1K 3M4 Canada
Phone: 403-329-2697 Fax: 403-329-2057 E-mail address: Adriana.predoicross@uleth.ca

Keywords: Temperature variable cell, spectroscopy, absorption, control software, laser spectroscopy, acetylene, nitrogen, spectral line shapes, dicke narrowing, pressure broadening, infrared spectroscopy, remote sensing, spectral line parameters

PACS: 33.20.-t, 33.20.Ea, 33.70.Jg , 32.70.Jz

ABSTRACT

Six nitrogen perturbed transitions of acetylene within the $\nu_1+\nu_3$ absorption band have been recorded using a 3-channel diode laser spectrometer. The goal being an improved understanding of both broadening and narrowing effects of low pressure acetylene under the influence of nitrogen gas. To this end we have examined C_2H_2 spectra using a hard collision Rautian profile over a range of five temperatures (213 K-333 K) and five pressures (5-40 Torr). From these fits we have obtained the N_2- broadening and narrowing coefficients of C_2H_2 and examined their temperature dependence. The experimentally measured narrowing coefficients have been used to estimate the nitrogen diffusion coefficients (D_{12}) and are presented within. The broadening coefficients and corresponding temperature dependence exponents have also been compared to that of calculations completed using a classical impact approach on an *ab initio* potential energy surface. We have observed a good agreement between our theoretical and experimental results.

For Review Only

1. INTRODUCTION

Accurate detailed knowledge of individual line parameters of the spectrum of acetylene is critical for the correct interpretation and modeling of many planetary atmospheres containing hydrocarbon molecules. The motivation behind this comes from our understanding that acetylene can be either a product or a reactant in many processes that are observed in planetary atmospheres [1-9]. Not only do we require good information about the self-interacting molecule but we also require an intimate understanding of perturbed interactions. One of the most important perturbers we can examine is nitrogen as this is a major constituent of many atmospheres such as Earth and Titan [7].

Table 1 shows a summary of the studies previously reporting on nitrogen perturbed acetylene to date. From the table it is easy to see that most of our information has come from studies focused on room temperature measurements [10-20]. However, there have been a handful of studies that examined other temperature ranges [21-29]. It is the examination of these temperature dependencies that are vital to improving our interpretation of atmospheric data, as most regions of the atmosphere are not at a constant temperature. Therefore by obtaining temperature dependence exponents for broadening, shift and narrowing we can improve radiative transfer models used to examine data collected from remote sensing observations.

Our choice of the particular line shape of interest we want to examine is also vital to improving our understanding of these transitions. It has been found that the Voigt profile, thought easy to fit does not always obtain the most accurate results [12, 14, 16, 24, 25, 27-30]. This is even more important when considering low pressure gas when collisional narrowing of the Doppler profile known as "Dicke narrowing" takes place [31]. The work presented here adopts the use of the hard collision Rautian line shape profile [32] to examine the temperature dependence of the N_2- broadening and narrowing coefficients.

Present experimental measurements are compared to theoretical calculation of the collisional linewidths. The calculations presented here are the first ones performed for this system on a true potential energy surface (PES). Indeed, very recently [33] a four dimensional *ab initio* PES has been determined for the C_2H_2-N_2 system. This PES has been computed using a supermolecular method in which the interaction energies are expressed as the difference between the energy of the complex and the energies of the monomers. Namely, the coupled cluster method at a single and double excitations level with triple excitations included perturbatively, i.e. CCSD(T), has been used.

2. EXPERIMENTAL DETAILS

All of the experimental data presented here were recorded using a 3-channel tunable diode laser spectrometer at the University of Lethbridge. A description of the setup and its functionality can be found in Ref [27]. The New Focus Velocity laser system provides a tunable range of 1.5 to 1.57 μm and can provide a signal-to-noise ratio better than 1000. This high S/N

For Review Only

has proven to be very useful when examining low pressure spectra [29]. The radiation from the laser is directed through two sample chambers. The first is a temperature and pressure controlled chamber with a path length of 1.54 cm where the mixture of N_2 and C_2H_2 was filled. The second is a slightly smaller chamber with the same path length. This chamber was filled with pure gas at room temperature and used as a calibration source.

The spectra of six transitions P(21), P(19), P(16), R(21), R(19), and R(16) belonging to the $\nu_1+\nu_3$ absorption band of acetylene were recorded. The gas used for the reference chamber was pure C_2H_2 provided by Praxair with a quoted concentration of 99.6%. The gas samples kept inside the temperature control chamber was also provided by Praxair and was quoted as being 9.94% C_2H_2 with the remaining being N_2. Low pressure tests on the P(11) transition in the $\nu_1+\nu_3$ band showed that the concentration was within 0.5% of the quoted value.

The spectra were recorded at the following temperatures 213, 253, 296, 313, and 333 K. For each set temperature we recorded spectra at 40, 30, 20, 10, and 5 Torr. The temperature of the temperature controlled chamber was monitored by an 8-channel Lakeshore (model 218) temperature monitor and controlled by a NesLab ULT 80 chiller. The gas samples pressures were monitored by two MKS Baratron capacitance manometers with full scale reading of 10 Torr and 100 Torr. The 10 Torr gauge was used for monitoring the gas pressures inside the reference chamber and the 100 Torr gauge was used to monitor the pressures inside the temperature controlled chamber. Once thermal equilibrium was reached the sample temperatures and pressures were stable to within ±0.3 K and ±0.1% during the course of each scan [27, 29]. Table 2 shows the experimental details for the R(21) transition with the other five transitions having very similar pressures and temperatures.

The recorded spectra were fit using a multispectral fitting routine [34]. This routine allows for simultaneous fitting of spectra at several different pressures for one set temperature. It also allows for the inclusion of an instrumental line shape (ILS) which is convolved with the spectral line shape of choice. In order to minimize any errors in our results we have used the same ILS as was previously discussed and verified in Ref [29]. The experimental errors associated with the measured broadening and narrowing coefficients are assumed to have the same values as those discussed in Ref [29], where we had found there to be an error no greater than 1% and 3% for our determined broadening and narrowing parameters respectively. Initial parameters for both self- and N_2- broadening, shift, and narrowing were obtained from Refs [28, 29]. The HITRAN database [35] was used for all line positions and intensities. Though not directly observed at the pressures measured here the effects due to line mixing were included within the fitting routine and were set to the values reported in Ref [27].

3. SPECTROSCOPIC LINE SHAPE ANALYSIS

When fitting recorded laboratory spectra it becomes very important to choose the appropriate line shape function that will mimic the physical conditions of the gas under examination. Typically for remote sensing purposes we use a Voigt line shape function which is

For Review Only

the convolution of a Lorentz and Doppler line shape function. The Voigt profile is a fast and reliable way to examine spectra of this nature. However, with the ever improving advances in signal-to-noise ratio for the new remote sensing instruments being developed the more subtle effects that were not noticeable in the past now influencing the errors in our results.

One such effect is known as "Dicke narrowing". This narrowing effect occurs at intermediate pressures when the mean free path of the molecules becomes equal to or less than the wavelength of the incident radiation. When this condition is met a simple Voigt profile will result in the retrieval of broadening coefficients that are smaller than what we would expect to observe. In order to account for this narrowing we can adopt a line shape function that includes the mechanisms of the Dicke narrowing effect.

To take into account for such an effect the soft and hard collision models are often used [32, 36]. Despite the physics leading to these models being very different, it was found for the case of self-perturbed spectrum of C_2H_2 [29] that there was no substantial difference in the residuals produced from fits of these two line shape functions to that of the experimental lineshape even though they did produce slightly different narrowing parameters. Generally, the choice of which line shape function to fit to the experimental lineshape comes down to the masses of the perturber and radiator, as was seen for the self-perturbed case [29] neither lineshape function was preferable. For the case of N_2 perturbed spectrum of C_2H_2 it was decided to only make use of an un-correlated hard collision Rautian line shape function as the mass of N_2 and C_2H_2 are very similar. Therefore fitting of the experimental lineshape function using the Galatry lineshape function was assumed to add no extra value to our analysis. Figure 1 shows the spectra of the P(16) line of the $\nu_1+\nu_3$ band measured at 40 Torr. In the figure one can see that when fitting with a Voigt profile we get a 'w'-type residual which is indicative of the broadening in the Dicke narrowing regime. It is clearly shown that once we fit the data using a diffusion profile such as the Rautian we get an improved result. It was found that for the spectra recorded at 333 K the percent difference between the obtained broadening coefficients using the Voigt and Rautian lineshape functions was as high as 6%. This difference in retrieved values diminished along with the temperature as we observed that at lower temperatures (i.e. 213 K) we had only 3% difference.

Below we present the expressions used to retrieve the N_2-broadened half-width and narrowing coefficients temperature dependences:

$$\gamma(p,T) = p\left[\gamma^{o}_{N_2}(p_o,T_o)(1-\chi)\left[\frac{T_o}{T}\right]^{n_1} + \gamma^{o}_{Self}(p_o,T_o)\chi\left[\frac{T_o}{T}\right]^{n_2}\right] \quad \textbf{(1)}$$

$$\beta(p,T) = p\left[\beta^{o}_{N_2}(p_o,T_o)(1-\chi)\left[\frac{T_o}{T}\right]^{n'_1} + \beta^{o}_{Self}(p_o,T_o)\chi\left[\frac{T_o}{T}\right]^{n'_2}\right] \quad \textbf{(2)}$$

For Peer Review Only

In equations (1) and (2) the reference pressure and temperature are p_o = 1 atm and T_o =296 K, respectively. $\gamma^o_{N_2}$ and $\beta^o_{N_2}$ are the retrieved N_2-broadened half-width and narrowing coefficients at the reference pressure p_o (1 atm) and reference temperature T_o (296 K). γ and β are the measured broadened half-width and narrowing coefficients of the spectral line at the total sample pressure of p and temperature T. The total sample pressure $p = p_{N_2}+p_{self}$ and χ is the ratio of p_{self} to p. n and n' are the temperature dependence exponents of the broadened half-width and narrowing coefficients. The use of equation (2) for examining the temperature dependence of the narrowing coefficient has been justified by the work of both Li *et al*. [37, 38] and Povey *et al.* [29]. It is important to note that equations (1) and (2) are merely approximations that will become less valid with increasing temperatures [39].

Using a hard collision Rautian line shape model we have examined the N_2- broadening and narrowing parameters for six transitions in the $\nu_1+\nu_3$ band of C_2H_2. The line parameters were obtained by using a weighted multispectrum analysis software [34]. For one set temperature multispectrum fits were performed on the set of spectra recorded for different pressures. The software uses a non-linear fitting routine to optimize the line parameters by minimizing the residual. For each line examined a simultaneous fit of the intensity, N_2-broadening and N_2-narrowing was completed. The shift was also fit simultaneously however due to the low pressures of the sample gas the results for the shift were not ideal for publication.

3.1. Modeled N_2-Broadend Line Width

In this work we calculate the linewidths of C_2H_2 infrared spectral lines (electric dipole absorption) broadened by N_2 in the frames of the classical impact approach of Gordon [40, 41] for isolated lines (no pressure-induced interference). To model translational and rotational motion of C_2H_2 and N_2 molecules we use 3D exact classical equations of motion which describe the collision of two rigid linear molecules.

The dynamics were performed on the four dimensional *ab initio* potential energy surface of Thibault et al [33]. For technical (and computing) reasons this PES has been developed, from 2 to 21 Å, over 85 bispherical harmonics [42, 43]. Such a large expansion is required because of the steepness of the repulsive part of the potential at short range: a region of major importance for the calculations of pressure broadening coefficients for temperature greater than about 100 K.

Classical calculations were done for three temperatures of the C_2H_2-N_2 mixture: 213 K, 296 K and 333 K and are shown in Figure 2. Exact classical 3D dynamics of C_2H_2-N_2 collisions was described by 17 first-order Hamilton differential equations in body-fixed coordinates [44]. Spin statistical weights of perturbing N_2 molecules were taken into account in usual way. Initial intermolecular distance was set large enough (15 Å) to exclude starting interaction between molecules. Other collision parameters (initial conditions for trajectory calculations) were selected via a Monte-Carlo procedure. Uniform sampling was applied to the directions of rotation and initial orientations of both molecules in 3D space. A very effective algorithm of impact parameter b sampling [45] was used in Monte-Carlo calculations which reduces the

For Review Only

computation time by half. The impact parameter was bracketed within the range of (0–12) Å. All the calculations were made using the approximation of mean thermal velocity (MTHV) which greatly reduces CPU time. In MTHV approximation all initial relative velocities of colliding molecules are set equal to their mean thermal relative velocity $\bar{v} = \sqrt{\frac{8k_B T}{\pi\mu}}$ associated with gas temperature (k_B being the Boltzmann constant and μ = 13.487, μ being the reduced mass of the C_2H_2-N_2 pair). The statistical error of calculated linewidths (i.e. RMS error of Monte-Carlo averaging over initial conditions of collisions) was kept for different values of temperature T and rotational quantum number J'' generally at the level less than 1%.

3.2. N_2-Broadening of Acetylene Transitions

Table shows the N_2-broadening coefficients measured for all five temperatures. A comparison of our experimental results to those of the theoretically determined line widths from section 3.1 can be seen in Figure 3. From the figure it can be seen that both sets of data agree with each other quite well with a maximum relative difference no greater than 7%.

Figure 4 shows the results of our room temperature N_2-broadening coefficients and a comparisons with previous measurements reported in the literature. As can be seen in the figure the linewidths that were retrieved in this study agree reasonably well with most of the previous work completed to date.

Using Equation (1) we have calculated the temperature dependence of the N_2-broadening coefficients. Both experimentally and theoretically determined N_2-broadening temperature dependence coefficients n are shown in Table 4 and plotted in Figure 5. In Figure 5 we compare our current results with those found by Rozario *et al.* [28] and Campbell *et al.* [26]. Our coefficients of line broadening temperature dependence n reasonably match previous work done for larger values of the quantum number $|m|$. We immediately notice that as $|m|$ becomes smaller we have more deviation from both the theoretical work presented in this paper and that of Campbell *et al.* [26]. However, it is important to note that the work done by Campbell *et al.* [26] where they have smoothed out their results agrees quite well with the proposed theoretical calculations presented here. From Figure 5 it can be seen that for the R-branch transitions we have much better agreement than we get for the P-branch transitions. It is our belief that the initial parameters used for the self-narrowing obtained from Ref [29] have allowed for less error to be introduced into the results obtained for the R-branch transitions. However, for the P-branch transitions we had to make the assumption that initial self-narrowing coefficients were similar to those obtained for the R-branch. At this moment we don't know of any published work showing both the m and temperature dependence of the self-narrowing coefficients for P-branch transitions.

3.3. N_2-Narrowing of Acetylene Transitions

For Review Only

In our previous study [29] we determined that only transitions recorded at pressures below 40 Torr were strictly in the Dicke narrowing regime. Therefore only spectra recorded at 40 Torr and below were recorded for this analysis. Figure 6 shows the relationship of the pressure dependent narrowing coefficient for the P(16) line of the $\nu_1+\nu_3$ band at 296 K plotted against the N_2 partial pressure of the chamber. It is clear from the figure that we have a linear relationship with pressure. This justifies our examination of the narrowing effects in this pressure region.

Table 5 shows the N_2-narrowing coefficients obtained from fitting the lineshape with the hard collision Rautian profile. The room temperature N_2-narrowing coefficients from Table 5 are compared in Figure 7 to the values obtained for both self- and N_2- narrowing by Povey *et al.* [29], McRaven *et al.* [14], Dhyne *et al.* [24, 25] and Valipour and Zimmermann [16]. From the figure we see that all studies report similar results. Each of the previous studies that examined both self- and N_2-narrowing [14, 16] report the N_2-narrowing coefficients to be smaller than the self-narrowing coefficients. This is what we also observe when we compare our previous work [29] with the present results.

The exponents n_1' for temperature dependence of N_2-narrowing are given in Table 5. These temperature dependence coefficients are plotted in Figure 8 along with self-narrowing temperature dependence coefficients from Ref [29]. From the figure it can be seen that the obtained temperature dependence is very similar and for the most part they agree to within one standard deviation of each other.

3.4. Diffusion Coefficients

Based on our previous study [29] we have equated the narrowing parameter $\beta^o_{N_2}$ to the dynamic friction coefficient β^o_{diff} in an attempt to estimate the nitrogen diffusion coefficient and its temperature dependence. The dynamic friction coefficient β^o_{diff} can be expressed by the following equation [37, 46]:

$$\beta^o_{diff} = \frac{k_B T}{2\pi m c D_{12}}, \tag{3}$$

Here k_B is the Boltzmann constant, T is the temperature in kelvin, m is the mass of acetylene molecule, c is the speed of light and D_{12} is the nitrogen diffusion coefficient for acetylene.

The mass diffusion coefficient for a gas mixture can be estimated in a general sense using the following equation [47, 48]:

$$D_{12} = \frac{\varepsilon_D k_B^{3/2}}{\sqrt{\pi}\, p \sigma_{12}^2 \Omega_{12}^{(1,1)}(T_{12})} \sqrt{T^3 \frac{(M_1 + M_2)}{2M_1 M_2}} \tag{4}$$

For Review Only

where M_1 and M_2 are the molecular weights of C_2H_2 and N_2 respectively, T is the temperature in kelvin, p is the pressure in atmospheres, $\varepsilon_D = 3/8$ as shown in [47]; T_{12} is a reduced temperature equal to k_BT/ε_{12}; ε_{12} is the depth of the isotropic potential and σ_{12} is the finite distance at which the intermolecular isotropic potential is zero. From the *ab initio* PES [33] values of ε_{12} = 88.8 cm^{-1} and σ_{12} = 4.015 Å were deduced and used. Finally, $\Omega_{12}^{(1,1)}$ is a dimensionless reduced collision integral, a function of the reduced temperature; values are tabulated in [47].

Using our obtained $\beta^o_{N_2}$ narrowing coefficients in equation (3) we calculated D_{12} for all the temperatures examined and have presented them in Table 6. The temperature dependence of the nitrogen diffusion coefficient was determined using equation (4) and was plotted in Figure 9. A comparison of the experimentally estimated, through equation (3), nitrogen diffusion coefficients to those obtained by equation (4) shows a similar trend in the temperature dependence of the nitrogen diffusion coefficients. However, unlike in our previous work [29] where it was determined that our diffusion coefficients were slightly lower than those obtained theoretically, we see that now our values are slightly larger than what is found using equation (4). This result indicates that $\beta^o_{diff} > \beta^o_{N_2}$ which implies that we found less narrowing as expected on the basis $\beta^o_{diff} = \beta^o_{N_2}$ .Such a result was also found in the work done by Wehr *et al* [49] for the CO-Ar system. We also should expect to see that for the P- and R- branch transitions the diffusion coefficients are similar (for a given m or J'' value). In Figure 9 we do in fact see this for the P(21) and R(21) transition. The fact that we don't see as close agreement between the P(16) and R(16) as well as the P(19) and R(19) may in fact be due to neighboring spectral features that are not properly accounted for as there are many weak transitions in this spectral region. However, it does indicate the need for a closer examination of both self- and N_2-narrowing coefficients for both P- and R- branch transitions on a larger scale than what is presented here.

Moreover, our comparison between the binary diffusion coefficients as given by equation (4) and our effective (or optical) diffusion coefficient retrieved by our lineshape analysis cannot be completely satisfactory for the following reasons. First, but this is not the main reason, equation (4) is a first order approximation [47, 50]. Secondly, paraphrasing Varghese and Hanson [51] "the two parameters (the mass diffusion constant and the effective diffusion coefficient) appear in different contexts in the theory and hence do not have the same physical significance…". More recently, Wehr *et al* [49] have also pointed out that both coefficients are related to (or take into account) different collisional mechanism (in addition, many studies found large discrepancies between these two kinds of coefficients, see Refs. in [49]). Therefore, one can only expect a rough agreement between these coefficients and such spectroscopic analysis can only provide an order of magnitude of the true binary diffusion coefficient.

For Review Only

4. CONCLUSION

Using a 3-channel tunable diode laser system we have for the first time examined the temperature dependence of N_2-narrowing coefficients for six transitions in the $\nu_1+\nu_3$ absorption band of acetylene. The N_2-broadening that was obtained while examining the hard collision Rautian line shape profile agrees very well with the theoretical calculations presented here. The full classical values calculated on the very first complete four-dimension *ab initio* PES [33] for the C_2H_2-N_2 system are very encouraging and will allow us to compare the methods for determining pressure broadening coefficients for this system like was recently done for similar systems (N_2-H_2, N_2-N_2, C_2H_2-H_2, see Refs [52-54]). In addition, careful comparisons of both our N_2- broadening and narrowing coefficients with previous studies have shown strong agreement with each other.

For a more physical interpretation of the narrowing effects in our low pressure spectra we should consider two main effects. The first one is the Dicke narrowing effect discussed in detail in this study. The second contribution to line narrowing arises from the effects of molecular speed-dependence on collisional line broadening. Using our software we were unable to quantify individual contributions to line narrowing. Any analysis that takes into account both Dicke narrowing and speed-dependent collisional broadening would have to be done carefully as to avoid any fitting error due to the highly correlated nature of these two effects.

For Review Only

Acknowledgements

This work was supported by the Natural Sciences and Engineering Research Council of Canada. We would like to further thank the AMETHYST program at the University of Lethbridge for their continued funding and academic support. We are grateful to Dr. Daniel R. Hurtmans of Universite Libre de Bruxelles for making available to us his line shape fitting software. Finally Chad Povey would like to thank his father, Rod Povey (who passed away during the writing of this document) for his long-time support and guidance.

References

[1] H.W. Moos, J.T. Clarke, *The Astrophysical Journal* 229 (1979) L107-L108.
[2] D. Cronn, E. Robinson, *Geophysical Research Letters* 6 (1979) 641-644.
[3] A. Goldman, F.J. Murcray, R.D. Blatherwick, J.R. Gillis, F.S. Bonomo, F.H. Murcray, D.G. Murcray, R.J. Cicerone, *Journal of Geophysical Research-Oceans and Atmospheres* 86 (1981) 2143-2146.
[4] R. Zander, C.P. Rinsland, D.H. Ehhalt, J. Rudolph, P. Demoulin, *Journal of Atmospheric Chemistry* 13 (1991) 359-372.
[5] J. Rudolph, A. Khedim, B. Bonsang, *Journal of Geophysical Research-Atmospheres* 97 (1992) 6181-6186.

[6] T. Fouchet, E. Lellouch, B. Bezard, H. Feuchtgruber, P. Drossart, T. Encrenaz, *Astronomy & Astrophysics* 355 (2000) L13-L17.
[7] A. Coustenis, R.K. Achterberg, B.J. Conrath, D.E. Jennings, A. Marten, D. Gautier, C.A. Nixon, F.M. Flasar, N.A. Teanby, B. Bezard, R.E. Samuelson, R.C. Carlson, E. Lellouch, G.L. Bjoraker, P.N. Romani, F.W. Taylor, P.G.J. Irwin, T. Fouchet, A. Hubert, G.S. Orton, V.G. Kunde, S. Vinatier, J. Mondellini, M.M. Abbas, R. Courtin, *Icarus* 189 (2007) 35-62.
[8] T. Kostiuk, T. Hewagama, K.E. Fast, T.A. Livengood, J. Armen, D. Buhl, G. Sonnabend, F. Schmulling, J.D. Delgado, R. Achterberg, *Planetary and Space Science* 58 (2010) 1715-1723.
[9] C.A. Nixon, R.K. Achterberg, P.N. Romani, M. Allen, X. Zhang, N.A. Teanby, P.G.J. Irwin, F.M. Flasar, *Planetary and Space Science* 58 (2010) 1667-1680.
[10] D. Lambot, G. Blanquet, J.P. Bouanich, *Journal of Molecular Spectroscopy* 136 (1989) 86-92.
[11] V.M. Devi, D.C. Benner, C.P. Rinsland, M.A.H. Smith, B.D. Sidney, *Journal of Molecular Spectroscopy* 114 (1985) 49-53.
[12] L. Fissiaux, M. Dhyne, M. Lepere, *Journal of Molecular Spectroscopy* 254 (2009) 10-15.
[13] S.W. Arteaga, C.M. Bejger, J.L. Gerecke, J.L. Hardwick, Z.T. Martin, J. Mayo, E.A. McIlhattan, J.M.F. Moreau, M.J. Pilkenton, M.J. Polston, B.T. Robertson, E.N. Wolf, *Journal of Molecular Spectroscopy* 243 (2007) 253-266.
[14] C.P. McRaven, M.J. Cich, G.V. Lopez, T.J. Sears, D. Hurtmans, A.W. Mantz, *Journal of Molecular Spectroscopy* 266 (2011) 43-51.
[15] A.S. Pine, *Journal of Quantitative Spectroscopy & Radiative Transfer* 50 (1993) 149-166.
[16] H. Valipour, D. Zimmermann, *Journal of Chemical Physics* 114 (2001) 3535-3545.
[17] J.P. Bouanich, D. Lambot, G. Blanquet, J. Walrand, *Journal of Molecular Spectroscopy* 140 (1990) 195-213.
[18] A. Babay, M. Ibrahimi, V. Lemaire, B. Lemoine, F. Rohart, J.P. Bouanich, *Journal of Quantitative Spectroscopy & Radiative Transfer* 59 (1998) 195-202.
[19] J.P. Bouanich, G. Blanquet, J. Walrand, *Journal of Molecular Spectroscopy* 203 (2000) 41-48.
[20] P. Minutolo, C. Corsi, F. D'Amato, M. De Rosa, *European Physical Journal D* 17 (2001) 175-179.
[21] P. Varanasi, *Journal of Quantitative Spectroscopy & Radiative Transfer* 47 (1992) 263-274.
[22] J.P. Bouanich, G. Blanquet, J.C. Populaire, J. Walrand, *Journal of Molecular Spectroscopy* 190 (1998) 7-14.
[23] G. Blanquet, J. Walrand, J.P. Bouanich, *Journal of Molecular Spectroscopy* 210 (2001) 1-7.
[24] M. Dhyne, L. Fissiaux, J.C. Populaire, M. Lepere, *Journal of Quantitative Spectroscopy & Radiative Transfer* 110 (2009) 358-366.
[25] M. Dhyne, P. Joubert, J.C. Populaire, M. Lepere, *Journal of Quantitative Spectroscopy & Radiative Transfer* 111 (2010) 973-989.
[26] N.T. Campbell, J.D. Cook, B.A. Coombs, E.P. Fuller, J.L. Hardwick, S.M. Hurley, L.K. Ho, P.A. Kovac, E.J. Robertson, E.N. Senning, J.K. Utterback, R.S. Wiser, *Molecular Physics* 109 (2011) 2199-2208.
[27] C. Povey, A. Predoi-Cross, D.R. Hurtmans, *Journal of Molecular Spectroscopy* 268 (2011) 177-188.

For Review Only

[28] H. Rozario, J. Garber, C. Povey, D. Hurtmans, J. Buldyreva, A. Predoi-Cross, *Molecular Physics* 110 (2012) 2645-2663.
[29] C. Povey, A. Predoi-Cross, D.R. Hurtmans, *Molecular Physics* 110 (2012) 2633-2644.
[30] F. Herregodts, D. Hurtmans, J. Vander Auwera, M. Herman, *Journal of Chemical Physics* 111 (1999) 7954-7960.
[31] R.H. Dicke, *Physical Review* 89 (1953) 472-473.
[32] S.G. Rautian, I.I. Sobelman, *Soviet Physics Uspekhi-Ussr* 9 (1967) 701-&.
[33] F. Thibault, O. Vieuxmaire, T. Sizun, B. Bussery-Honvault, *Molecular Physics* 110 (2012) 2761-2771.
[34] D. Hurtmans, G. Dufour, W. Bell, A. Henry, A. Valentin, C. Camy-Peyret, *Journal of Molecular Spectroscopy* 215 (2002) 128-133.
[35] L.S. Rothman, I.E. Gordon, A. Barbe, D.C. Benner, P.E. Bernath, M. Birk, V. Boudon, L.R. Brown, A. Campargue, J.P. Champion, K. Chance, L.H. Coudert, V. Dana, V.M. Devi, S. Fally, J.M. Flaud, R.R. Gamache, A. Goldman, D. Jacquemart, I. Kleiner, N. Lacome, W.J. Lafferty, J.Y. Mandin, S.T. Massie, S.N. Mikhailenko, C.E. Miller, N. Moazzen-Ahmadi, O.V. Naumenko, A.V. Nikitin, J. Orphal, V.I. Perevalov, A. Perrin, A. Predoi-Cross, C.P. Rinsland, M. Rotger, M. Simeckova, M.A.H. Smith, K. Sung, S.A. Tashkun, J. Tennyson, R.A. Toth, A.C. Vandaele, J. Vander Auwera, *Journal of Quantitative Spectroscopy & Radiative Transfer* 110 (2009) 533-572.
[36] L. Galatry, *Physical Review* 122 (1961) 1218.
[37] H. Li, A. Farooq, J.B. Jeffries, R.K. Hanson, *Applied Physics B-Lasers and Optics* 89 (2007) 407-416.
[38] H. Li, A. Farooq, J.B. Jeffries, R.K. Hanson, *Journal of Quantitative Spectroscopy & Radiative Transfer* 109 (2008) 132-143.
[39] J. Bonamy, D. Robert, C. Boulet, *Journal of Quantitative Spectroscopy & Radiative Transfer* 31 (1984) 23-34.
[40] R.G. Gordon, *Journal of Chemical Physics* 44 (1966) 3083.
[41] R.G. Gordon, *Journal of Chemical Physics* 45 (1966) 1649.
[42] L. Gomez, R.Z. Martinez, D. Bermejo, F. Thibault, P. Joubert, B. Bussery-Honvault, J. Bonamy, *Journal of Chemical Physics* 126 (2007).
[43] F. Thibault, B. Corretja, A. Viel, D. Bermejo, R.Z. Martinez, B. Bussery-Honvault, *Physical Chemistry Chemical Physics* 10 (2008) 5419-5428.
[44] S.V. Ivanov, O.G. Buzykin, *Molecular Physics* 106 (2008) 1291-1302.
[45] S. Chapman, S. Green, *Journal of Chemical Physics* 67 (1977) 2317-2331.
[46] M. Lepere, A. Henry, A. Valentin, C. Camy-Peyret, *Journal of Molecular Spectroscopy* 208 (2001) 25-31.
[47] J.O. Hirschfelder, C.F. Curtiss, R.B. Bird, Wiley-Interscience, 1964, p 1280.
[48] F. Thibault, A.W. Mantz, C. Claveau, A. Henry, A. Valentin, D. Hurtmans, *Journal of Molecular Spectroscopy* 246 (2007) 118-125.
[49] R. Wehr, R. Ciurylo, A. Vitcu, F. Thibault, J.R. Drummond, A.D. May, *Journal of Molecular Spectroscopy* 235 (2006) 54-68.
[50] F.R.W. McCourt, J.J.M. Beenaker, W.E. Köhler, I. Kučšer, Non equilibrium phenomena in polyatomic gases. Clarendon Press, Oxford, 1990.
[51] P.L. Varghese, R.K. Hanson, *Applied Optics* 23 (1984) 2376-2385.
[52] F. Thibault, S.V. Ivanov, O.G. Buzykin, L. Gomez, M. Dhyne, P. Joubert, M. Lepere, *Journal of Quantitative Spectroscopy & Radiative Transfer* 112 (2011) 1429-1437.

For Review Only

[53] L. Gomez, S.V. Ivanov, O.G. Buzykin, F. Thibault, *Journal of Quantitative Spectroscopy & Radiative Transfer* 112 (2011) 1942-1949.
[54] F. Thibault, L. Gomez, S.V. Ivanov, O.G. Buzykin, C. Boulet, *Journal of Quantitative Spectroscopy & Radiative Transfer* 113 (2012) 1887-1897.

For Review Only

Table captions

Table 1: Summary of previous studies examining acetylene broadened by N_2.

Table 2: Sample of experimental conditions for the R(21) transition.

Table 3: N_2-Broadening coefficients for five different temperatures obtained using an uncorrelated hard collision Rautian line shape model. The normal convention of $m = -J''$ for the P branch and $m = J''+1$ for the R branch is used.

Table 4: Comparison of theoretical and experimental results obtained for N_2-broadening coefficients at 296 K and temperature dependence exponents n_1.

Table 5: N_2-Narrowing coefficients for the five recorded temperatures using an uncorrelated hard collision Rautian line shape model. The last column shows the temperature dependence terms obtained from the data in the table and equation (2).

Table 6: Estimated N_2-Diffusion coefficients obtained from equation (3).

Figure captions

Figure 1: Observed and calculated spectra for the P(16) transition of the $\nu_1+\nu_3$ absorption band of C_2H_2 at a pressure of 40 Torr and temperature of 296 K. The residuals have been shifted and magnified for easier comparison.

Figure 2: Classically calculated 3D pressure broadening coefficients at the 3 temperatures studied.

Figure 3: Comparison of classically calculated and experimentally determined N_2-broadening coefficients for three different temperatures. In each panel the line depicts the theoretically determined broadening coefficients.

Figure 4: Panel A shows a comparison of the present N_2-broadening coefficients with previous studies. Panel B shows a smaller region between m=10 to m=25 where only values obtained from a narrowing model are compared.

Figure 5: Temperature dependence exponents n_1 obtained from equation (1).

Figure 6: The pressure dependent narrowing coefficient β_{N_2} for the P(16) and R(16) transitions at 296 K as they vary with the partial N_2 pressure.

Figure 7: Comparison of the N_2-Narrowing coefficients obtained at 296 K to previous work.

Figure 8: Narrowing temperature dependence coefficient n_1' obtained from equation (2). The diamonds show the results from our previous work [29] with self-narrowing coefficients.

Figure 9: Estimated diffusion coefficients obtained from retrieved experimental $\beta^o_{N_2}$ and equation (4)(3).

For Review Only

Vibrational Band	Broadener	Temperatures (K)	Assignment range	Ref.
ν_5	N_2, O_2	297	P(29)-R(25)	[10]
ν_5	N_2, O_2	297	P(35)-R(34)	[17]
ν_5	H_2, N_2,He, Ar	147-295	P(8)-R(21)	[21]
ν_5	H_2, N_2,He, Ar	296	R(3)-R(34)	[18]
ν_5	N_2	173.4	P(29)-R(28)	[22]
$\nu_4+\nu_5-\nu_4$	N_2,He	296	Q(1)-Q(35)	[19]
$2\nu_5-\nu_5$	N_2,He	296	Q(1)-Q(35)	[19]
$\nu_4+\nu_5-\nu_4$	N_2,He	183.2,198.2	Q(1)-Q(35)	[23]
$2\nu_5-\nu_5$	N_2,He	183.2,198.2	Q(1)-Q(35)	[23]
$\nu_4+\nu_5$	N_2, air	296	P(31)-R(20)	[11]
$\nu_4+\nu_5$	N_2	173.2-273.2	P(1)-R(23)	[24]
$\nu_4+\nu_5$	N_2	298	P(17)-R(22)	[12]
$\nu_4+\nu_5$	N_2	173.2-298.2	R(11)-P(23)	[25]
$\nu_1+\nu_3$	H_2, N_2,D_2, air	295	P(31)-R(27)	[13]
$\nu_1+\nu_3$	C_2H_2, N_2	296	P(11)	[14]
$\nu_1+\nu_3$	N_2	195, 373, 473	P(25)-R(25)	[26]
$\nu_1+\nu_3$	N_2, O_2, CO_2	296	P(26)-P(22)	[20]
$\nu_1+\nu_3$	N_2	213-333	P(31)-R(33)	[28]
$\nu_1+\nu_5$	C_2H_2, N_2, Ar	296	R(0)-R(7),Q(7)-Q(29)	[15]
$\nu_1+3\nu_3$	N_2, O_2,He, Ar, Ne, Kr, Xe	298	P(17)-R(22)	[16]

For Review Only

Sample of Experimental Conditions for the R(21) Transition			
Line	**Temperature (K)**	**Pressure (Torr)**	**# of Recorded Spectra**
R(21)	213.9(3)	5.214(5)	4
		10.214(10)	4
		20.270(20)	4
		30.408(30)	4
		42.371(42)	3
	253.4(3)	5.267(5)	4
		10.668(11)	4
		20.131(20)	4
		30.185(30)	4
		40.409(40)	4
	295.8(3)	5.264(5)	4
		10.324(10)	4
		19.839(20)	4
		30.013(30)	4
		40.364(40)	4
	312.7(3)	5.170(5)	4
		10.250(10)	4
		19.910(20)	4
		30.087(30)	4
		39.286(39)	4
	332.5(3)	5.499(5)	4
		10.898(11)	4
		21.153(21)	4
		29.983(30)	4
		40.022(40)	2

For Review Only

Retrieved N_2-Broadening Coefficients $\gamma^{\rho}_{N_2}$ (cm^{-1} atm^{-1})							
Line	**m**	**Line Position (cm^{-1})**	**213 K**	**253 K**	**296 K**	**313 K**	**333 K**
P(21)	-21	6501.7047	0.0888(9)	0.0798(8)	0.0708(7)	0.0692(7)	0.0665(7)
P(19)	-19	6507.3982	0.0947(9)	0.0832(8)	0.0769(8)	0.0719(7)	0.0704(7)
P(16)	-16	6515.7516	0.1017(10)	0.0889(9)	0.0774(8)	0.0766(8)	0.0714(7)
R(16)	17	6592.5030	0.0985(10)	0.085(9)	0.0752(8)	0.0727(7)	0.0699(7)
R(19)	20	6598.0774	0.0913(9)	0.0823(8)	0.0739(7)	0.0725(7)	0.0673(7)
R(21)	22	6601.6617	0.0859(9)	0.0768(8)	0.0693(7)	0.0689(7)	0.0676(7)

For Review Only

Retrieved N_2-Broadening Coefficients (cm^{-1} atm^{-1}) at 296 K and Determined Temperature Dependence Exponents							
Line	**m**	**Rautian $\gamma^0_{N_2}$**	**Calculated $\gamma^0_{N_2}$**	**% Difference**	**Rautian n_1**	**Calculated n_1**	**% Difference**
P(21)	-21	0.0708(7)	0.0736	3.77%	0.66(2)	0.57	12.87%
P(19)	-19	0.0769(8)	0.0775	0.80%	0.67(4)	0.60	9.30%
P(16)	-16	0.0774(8)	0.0815	5.02%	0.78(4)	0.67	13.66%
R(16)	17	0.0752(8)	0.0798	5.73%	0.77(2)	0.67	12.94%
R(19)	20	0.0739(7)	0.0757	2.35%	0.66(4)	0.60	7.97%
R(21)	22	0.0693(7)	0.0717	3.37%	0.55(5)	0.57	3.35%

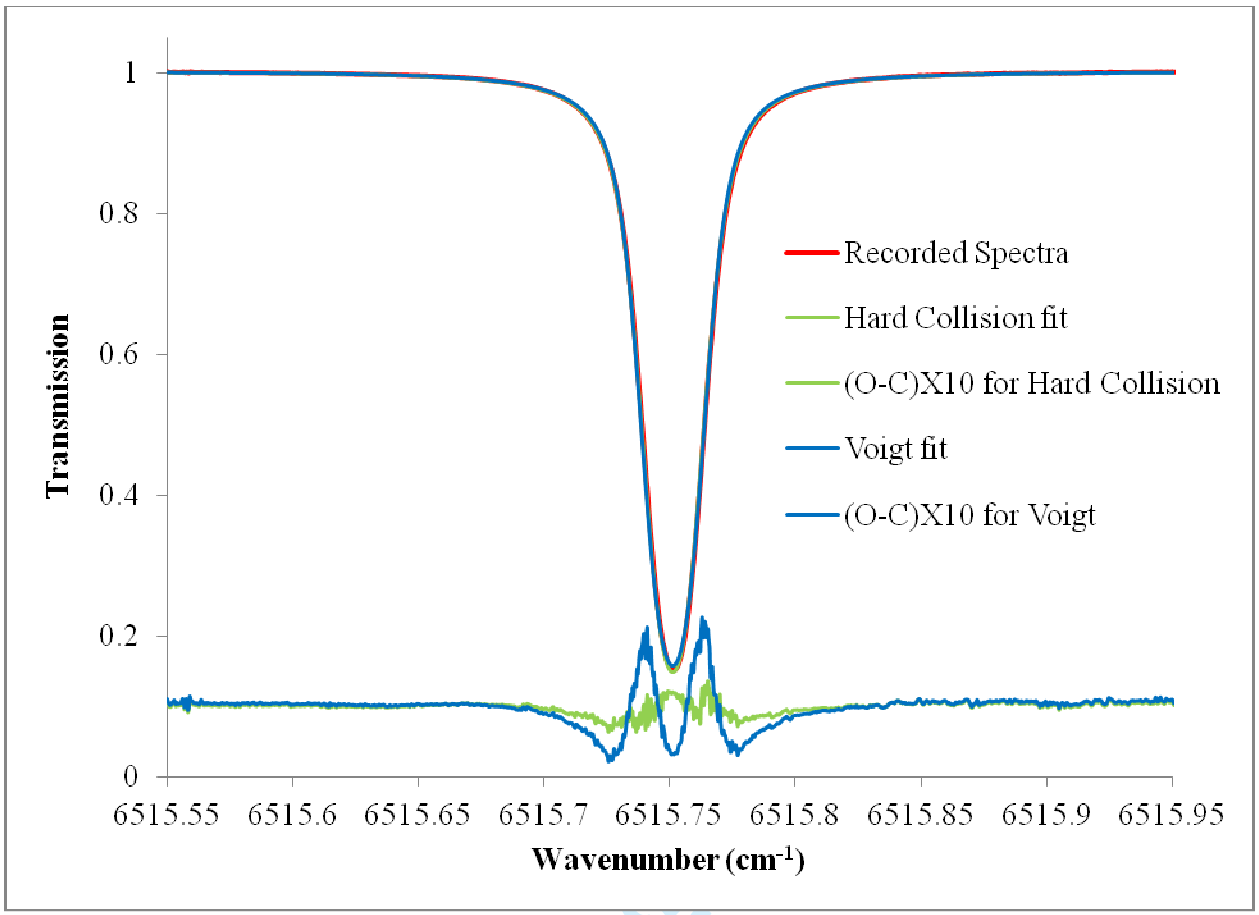
For Review Only

Retrieved N_2-Narrowing Coefficients $\beta^o_{N_2}$ (cm^{-1} atm^{-1}) and Temperature Dependence n_1'							
Line	**m**	**213 K**	**253 K**	**296 K**	**313 K**	**333 K**	**n_1'**
P(21)	-21	0.0279(9)	0.0225(7)	0.0182(6)	0.0177(6)	0.017(5)	1.146(78)
P(19)	-19	0.0273(9)	0.0232(7)	0.0184(6)	0.018(6)	0.0173(6)	1.076(81)
P(16)	-16	0.0256(8)	0.0239(8)	0.0217(7)	0.021(7)	0.0203(6)	0.533(26)
R(16)	17	0.0212(7)	0.0186(6)	0.0165(5)	0.0157(5)	0.015(5)	0.773(9)
R(19)	20	0.0211(7)	0.0188(6)	0.017(5)	0.016(5)	0.0153(5)	0.721(29)
R(21)	22	0.0225(7)	0.0209(7)	0.0187(6)	0.0173(6)	0.0163(5)	0.719(82)

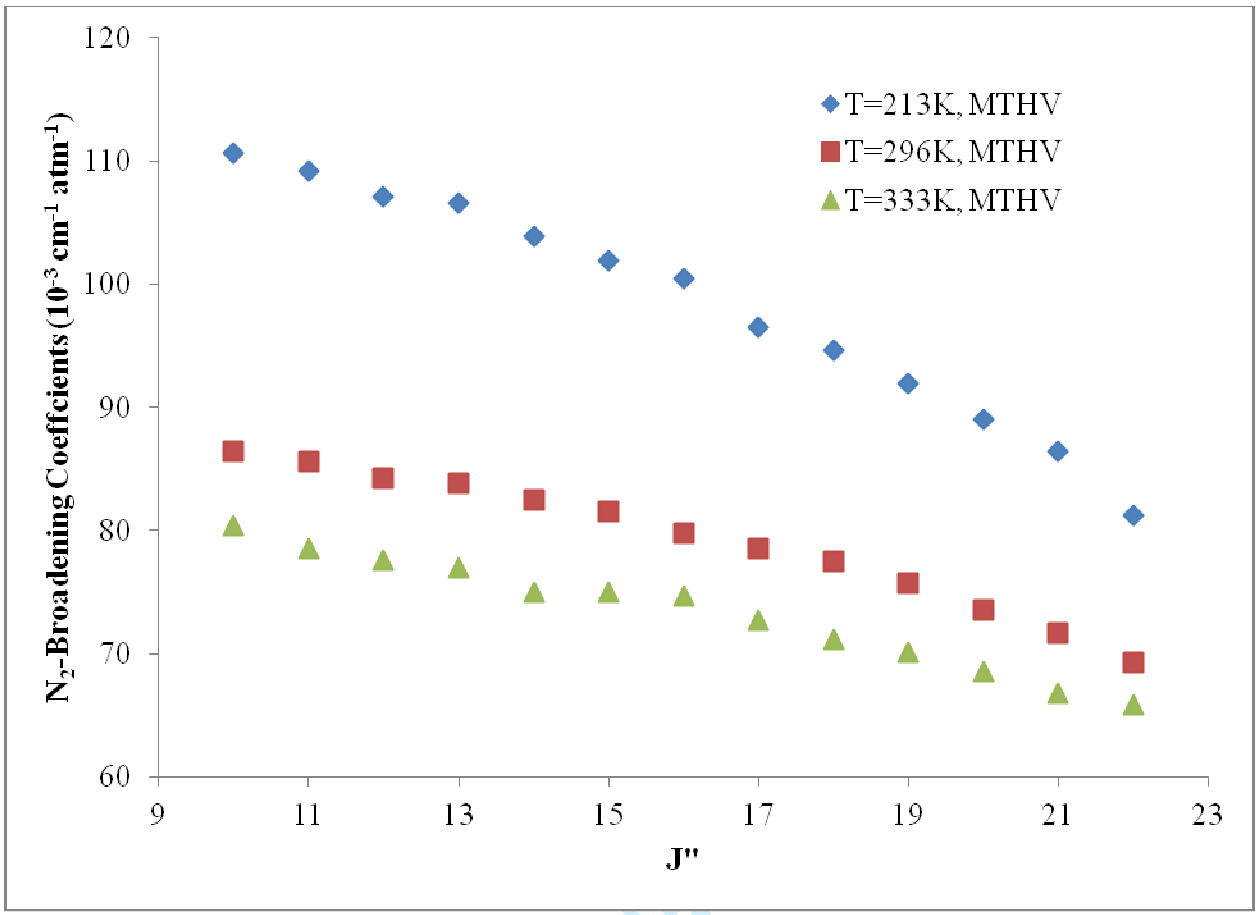
For Review Only

Retrieved N_2-Diffusion Coefficients D_{12} (cm^2 sec^{-1})							
Line	**m**	**213 K**	**253 K**	**296 K**	**% Difference**	**313 K**	**333 K**
P(21)	-21	0.129(4)	0.190(6)	0.275(9)	43.37%	0.300(10)	0.331(11)
P(19)	-19	0.132(4)	0.185(6)	0.272(9)	42.74%	0.295(9)	0.326(10)
P(16)	-16	0.141(5)	0.179(6)	0.232(7)	32.77%	0.253(8)	0.278(9)
R(16)	17	0.170(5)	0.231(7)	0.304(10)	48.73%	0.338(11)	0.376(12)
R(19)	20	0.171(5)	0.228(7)	0.295(9)	47.22%	0.332(11)	0.370(12)
R(21)	22	0.160(5)	0.206(7)	0.268(9)	41.82%	0.307(10)	0.345(11)

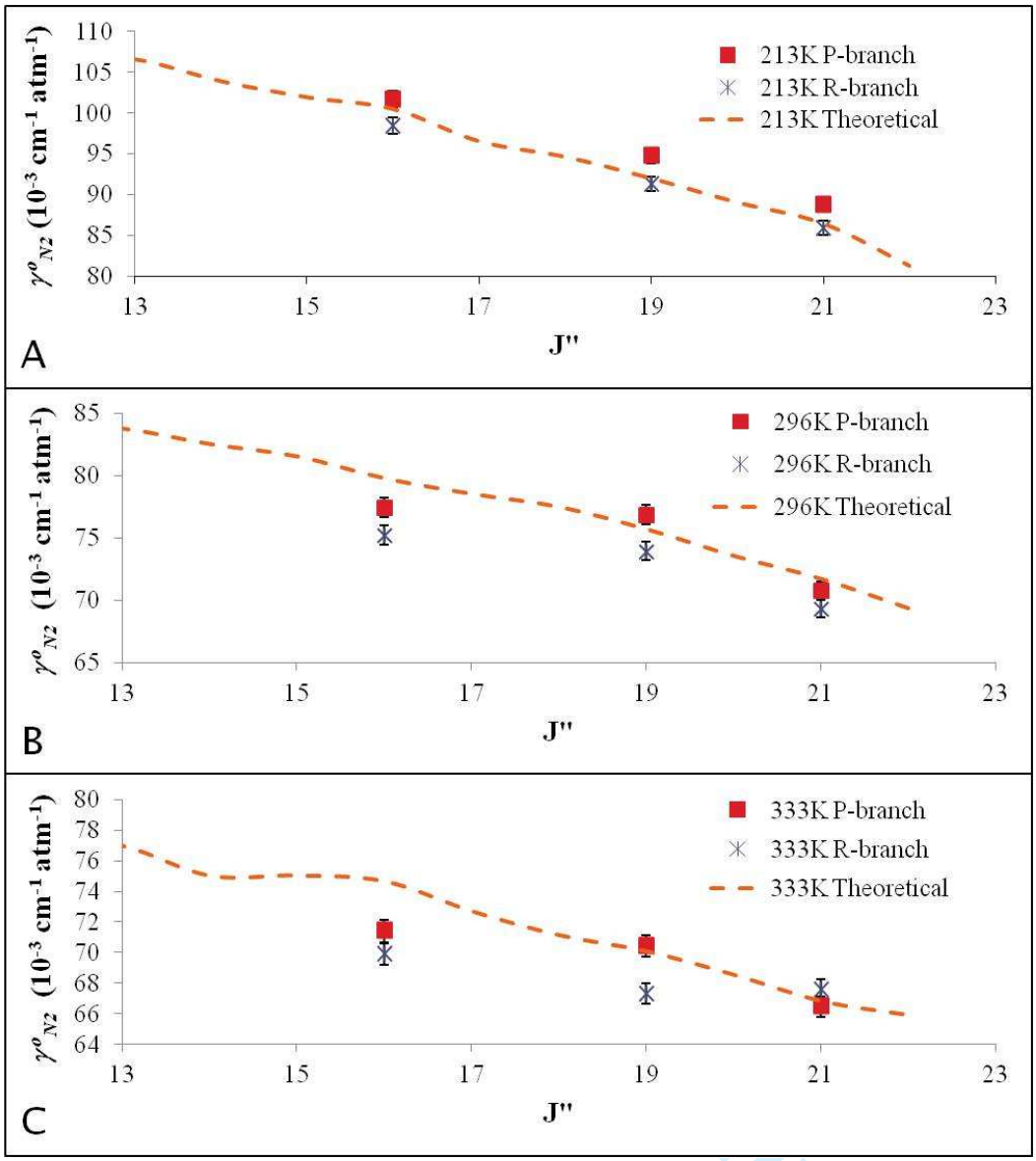
For Review Only

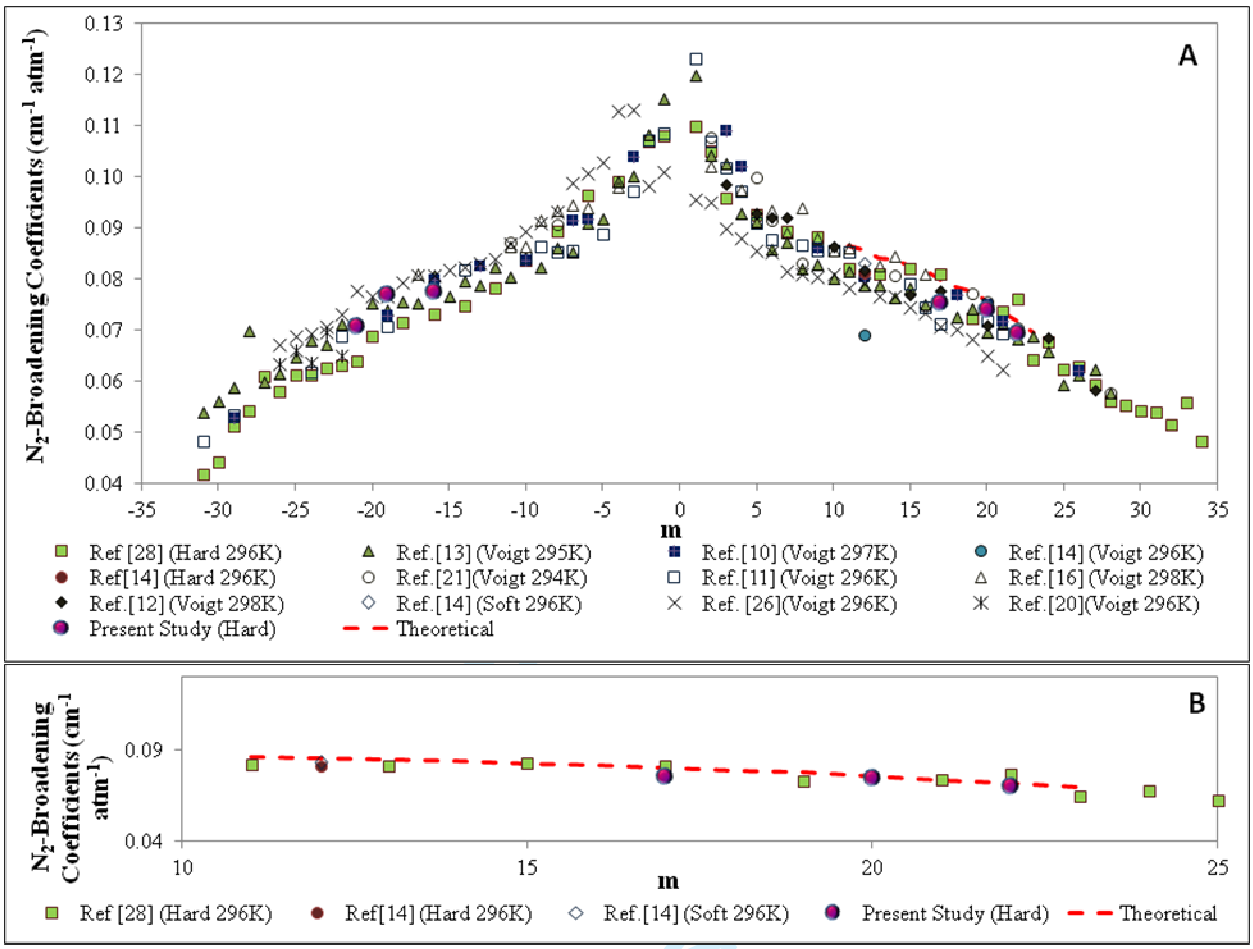


For Review Only

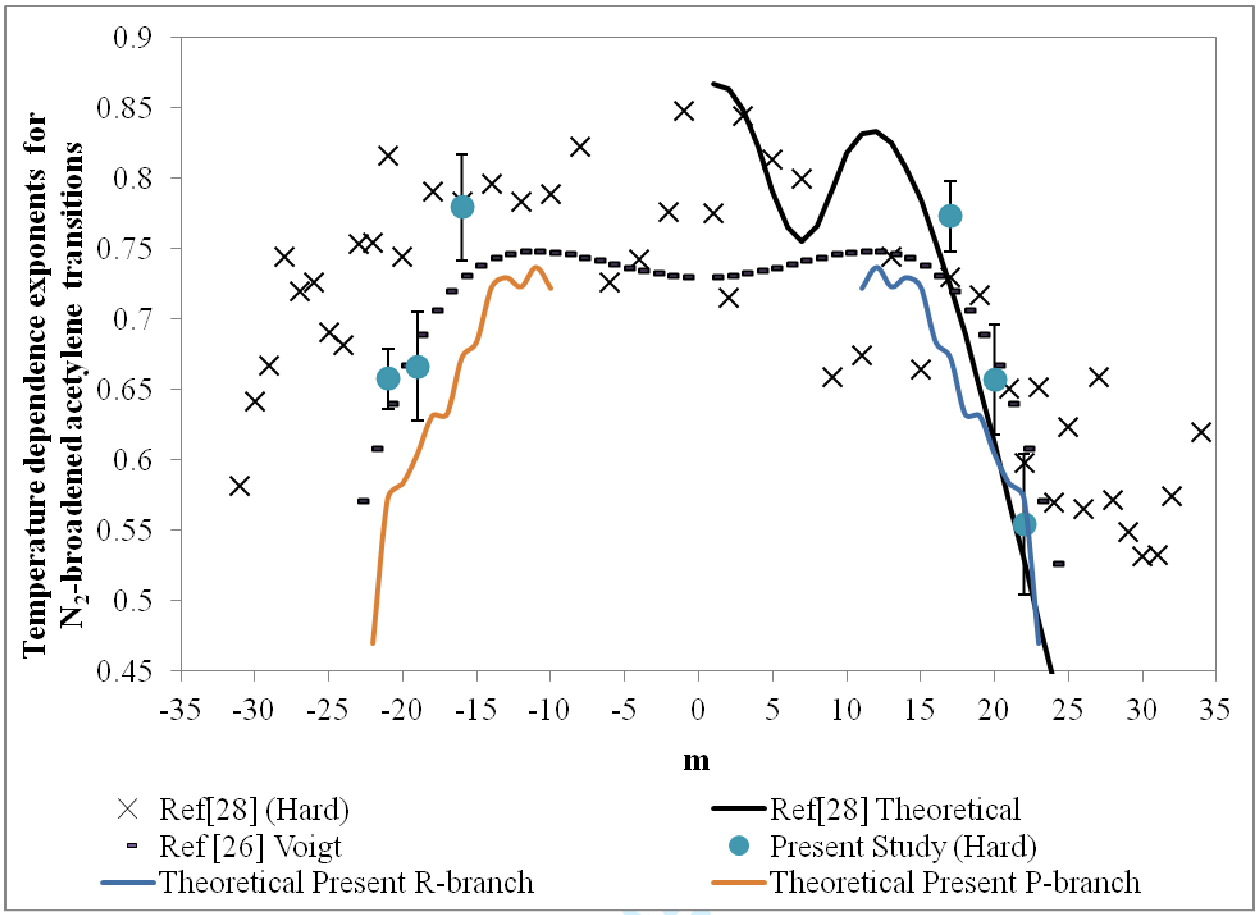


For Review Only

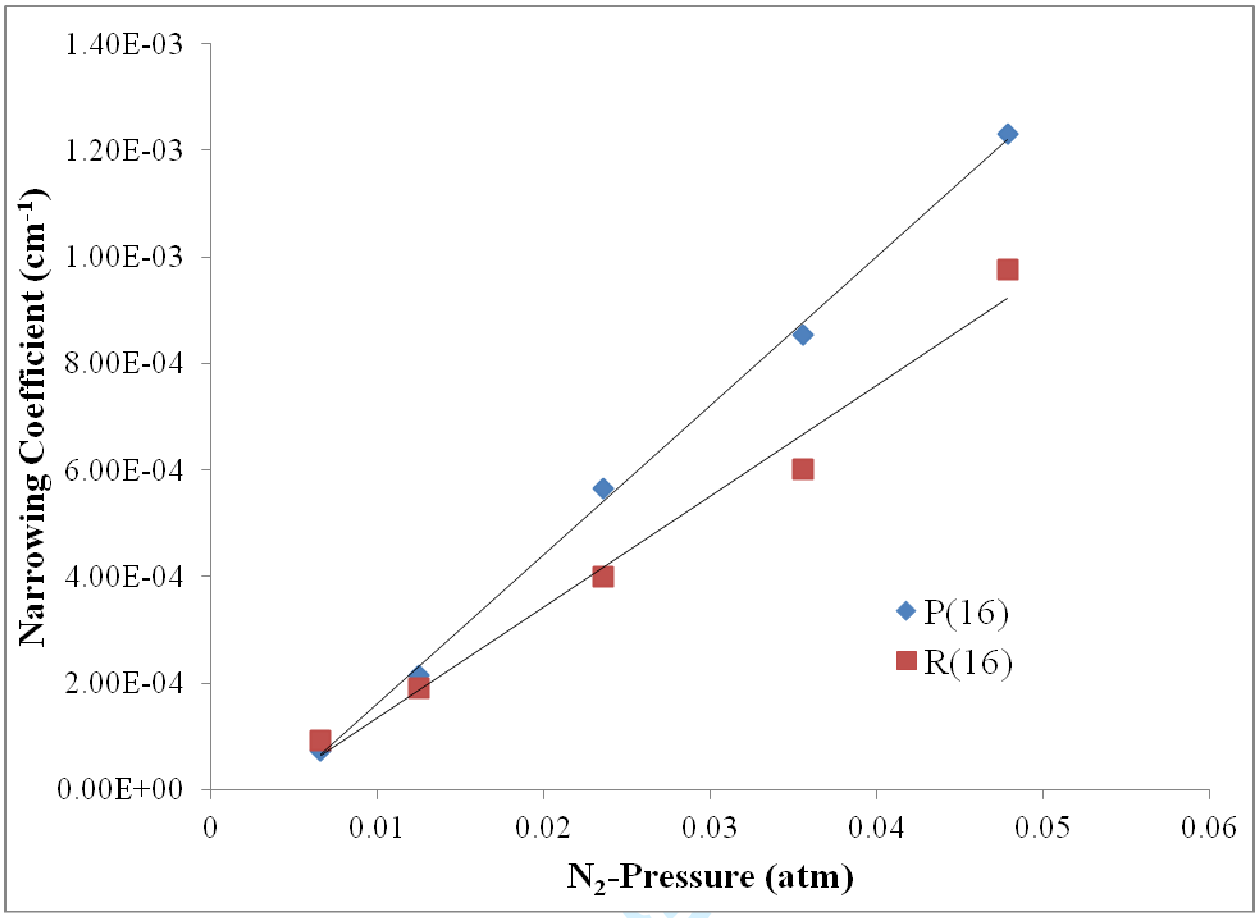

110
105
100
95
90
85
80
γ^o_{N2} (10^{-3} cm^{-1} atm^{-1})
13
15
17
19
21
23
J"
213K P-branch
213K R-branch
213K Theoretical
A
85
80
75
70
65
296K P-branch
296K R-branch
296K Theoretical
B
80
78
76
74
72
70
68
66
64
333K P-branch
333K R-branch
333K Theoretical
C



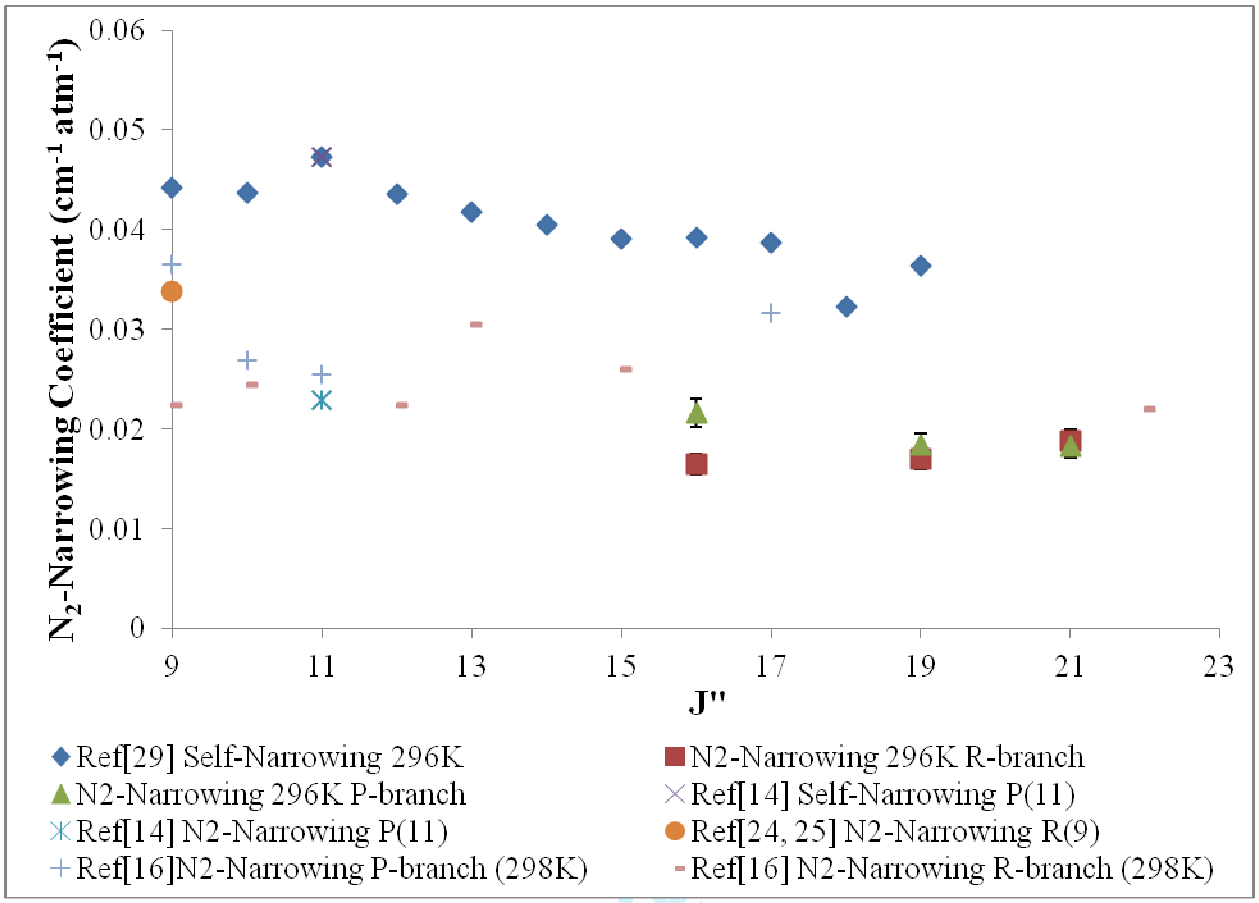
For Peer Review Only



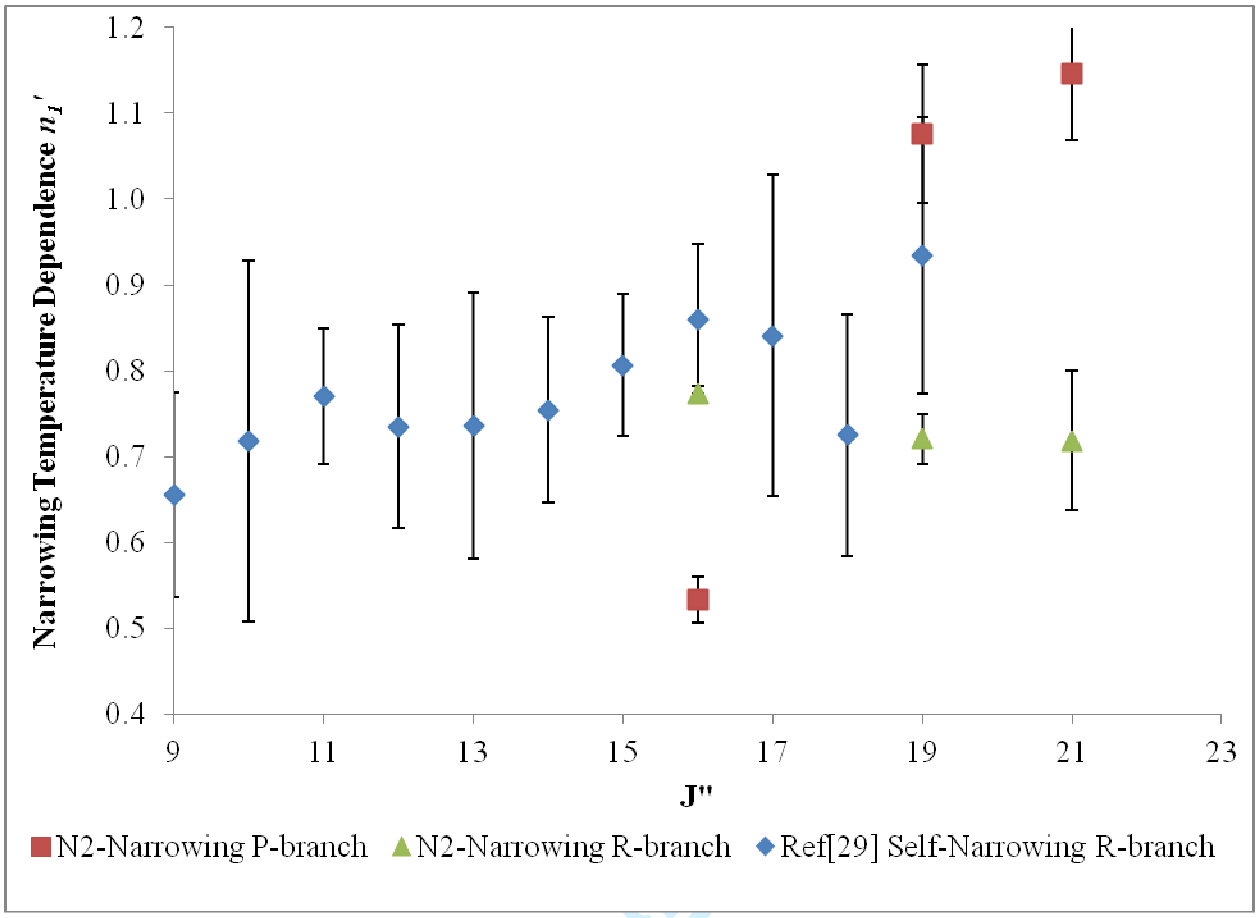
For Review Only



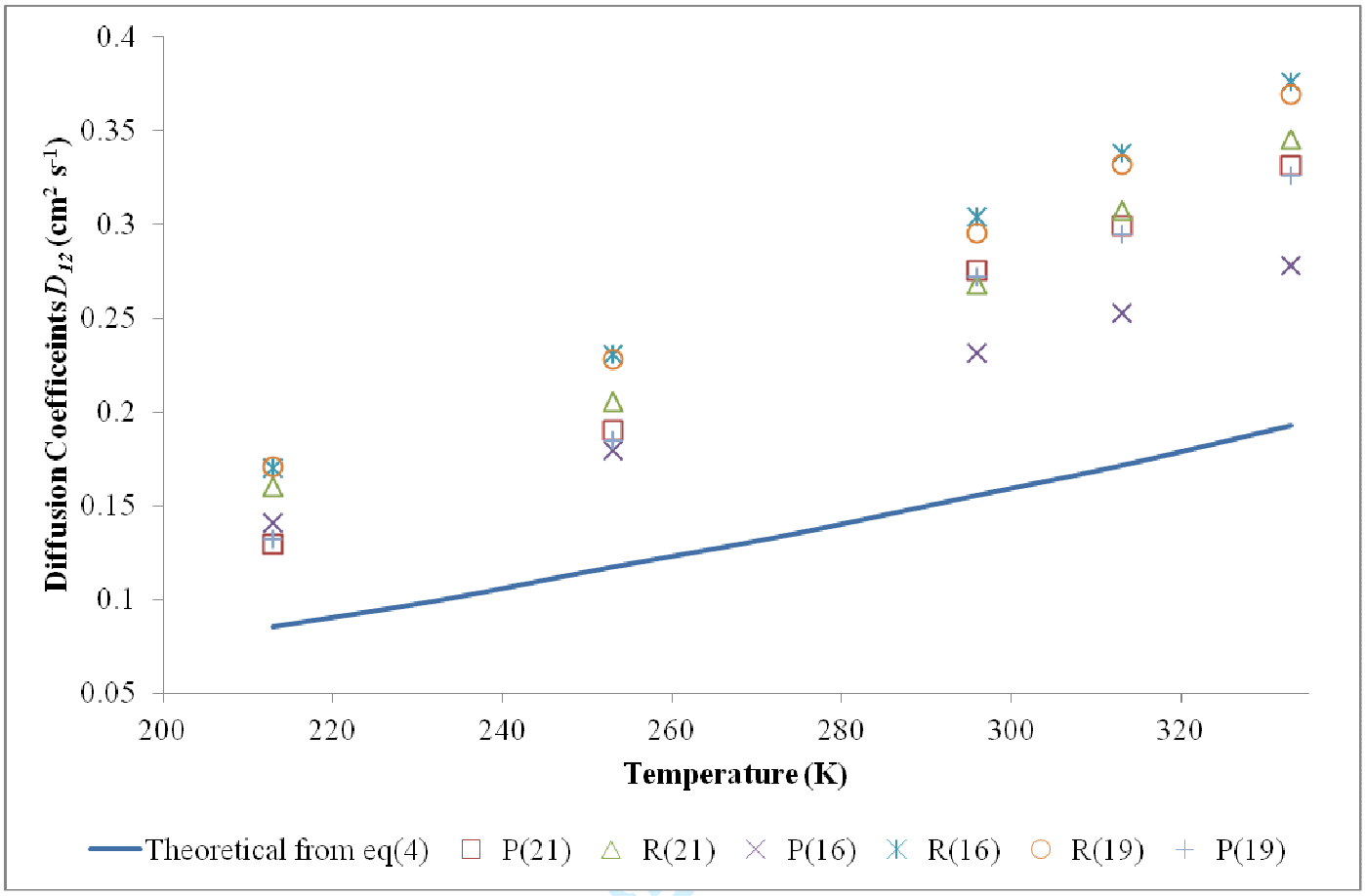
For Review Only



For Review Only



For Review Only



For Review Only